

Spin- $\frac{1}{2}$ Heisenberg antiferromagnet on the *kagomé* Lattice: High-temperature expansion and exact-diagonalization studies

N. Elstner and A. P. Young

Physics Department, University of California, Santa Cruz, California 95064

(Received 18 April 1994)

For the spin- $\frac{1}{2}$ Heisenberg antiferromagnet on the *kagomé* lattice we calculate the high-temperature series for the specific heat and the structure factor. A comparison of the series with exact-diagonalization studies shows that the specific heat has further structure at lower temperature in addition to a high-temperature peak at $T \approx \frac{2}{3}$. At $T = 0.25$ the structure factor agrees quite well with results for the ground state of a finite cluster with 36 sites. At this temperature the structure factor is less than two times its $T = \infty$ value and depends only weakly on the wave vector \mathbf{q} , indicating the absence of magnetic order and a correlation length of less than one lattice spacing. The uniform susceptibility has a maximum at $T \approx \frac{1}{6}$ and vanishes exponentially for lower temperatures.

I. INTRODUCTION

For a long time it has been speculated that low-dimensional quantum spin antiferromagnets may have magnetically disordered ground states. Most attention has been focused on the spin- $\frac{1}{2}$ Heisenberg antiferromagnet (HAFM) on the square lattice due to the close relation of this model with the problem of high-temperature superconductivity. However, it is now well established that the HAFM on this particular lattice has an ordered ground state.¹ The first system for which a disordered ground state was proposed is the HAFM on the triangular lattice.² In recent years this model has been the subject of intensive numerical investigations. Although most results indicate that the system remains ordered at $T = 0$, it seems that the sublattice magnetization and the spin stiffness are significantly smaller than for the square lattice.³⁻⁶

So far the best candidate for a magnetically disordered system is the *kagomé* structure: a triangular lattice with a triangular basis. The vectors of the underlying triangular Bravais lattice are

$$\mathbf{e}_1 = 2(1, 0), \quad \mathbf{e}_2 = (1, \sqrt{3}), \quad (1)$$

while basis vectors indicating the coordinates of the three sites in the triangular unit cell are

$$\mathbf{b}_1 = (0, 0), \quad \mathbf{b}_2 = (1, 0), \quad \mathbf{b}_3 = \left(\frac{1}{2}, \frac{\sqrt{3}}{2}\right). \quad (2)$$

The units are chosen so that the nearest neighbor distance equals unity. The structure is shown in Fig. 1. Because the *kagomé* lattice is not a Bravais lattice, but has three sites per unit cell, the structure factor is a 3×3 matrix.

Classical spins on the *kagomé* structure are frustrated, as they are on the triangular lattice, but the coordination number is smaller (4 for the *kagomé* structure instead of

6 for the triangular lattice). Even more important may be another difference: While the ground state on the triangular lattice is degenerate only with respect to global rotations in spin space, the classical ground states on the *kagomé* lattice have a local degeneracy, which results in a finite ground state entropy. Fluctuations around magnetically ordered states have a dispersionless zero-energy mode.⁷

Numerical studies using series expansions⁵ and exact-diagonalization techniques^{8,9} have convincingly shown that the ground state of the spin- $\frac{1}{2}$ HAFM on the *kagomé* lattice has no long range magnetic order. The exact-diagonalization studies^{8,9} find a very rapid decay of the spin-spin correlations indicating a correlation length ξ of only about one lattice spacing and a finite spin gap $\Delta \approx 0.25J$. There exist a number of proposals for a disordered ground state.¹⁰⁻¹² Large- N expansions for the $SU(N)$ and $Sp(N/2)$ generalizations^{11,12} of the HAFM predict a ground state with spin-Peierls order for $SU(N)$ or a spin liquid for $Sp(N/2)$. Up to now there exist no results from numerical calculations that confirm or contradict any of these proposals.

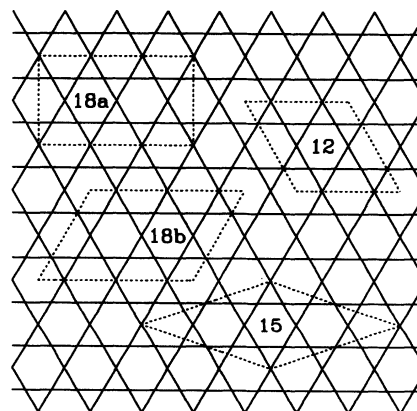


FIG. 1. The *kagomé* lattice with the finite clusters used in exact-diagonalization studies of the specific heat.

Apart from being a theoretical toy model for a disordered quantum spin system there exists at least one possible realization of the spin- $\frac{1}{2}$ HAFM on the *kagomé* structure: the second layer of ^3He atoms absorbed onto graphite at a particular coverage.¹⁰ It is, however, possible that this is too simple a model and a realistic description should include other spin-exchange interactions.¹³ Experiments on this system found a peak in the specific heat,¹⁴ but the total change in entropy per site between $T = \infty$ and an extrapolated value for $T = 0$ accounts for only one-half of $\ln(2)$ the expected value for an $S = \frac{1}{2}$ system. This suggests that there is a large number of low-lying states, which could contribute to additional structure, such as a second peak, in the specific heat at very low temperatures.

Exact diagonalization of a 12-site cluster¹⁰ on the *kagomé* lattice and simulations using the decoupled-cell Monte Carlo technique⁸ found such a peak. Simulations of larger systems¹⁵ using the forced oscillator method found only one high-temperature peak and an almost linear T dependence of the specific heat at temperatures below this single maximum. Based on this observation it was concluded that the double-peak structure reported for the 12-site system is due to finite size effects.

Further insight in the behavior of the system can be gained by calculating finite temperature properties. However, the most powerful technique, quantum Monte Carlo simulations, breaks down due to the sign problem for frustrated spin systems. In this paper we, therefore, follow a different approach and present results from high-temperature expansions as well as exact-diagonalization studies.

Section II contains the results for the specific heat, for which the series has been calculated up to 16th order in $J/k_B T$. We analyze the series using the method of Padé approximants and compare the results with data from exact-diagonalizations studies. Based on entropy arguments we will show that the low-temperature structure of the specific heat occurring in the finite cluster calculations¹⁰ cannot be a spurious finite size effect. In the third section we present results for the spin-spin correlation function, which has been calculated up to 14th order in $J/k_B T$. Extrapolations give quantitative results down to $T \approx 0.25J/k_B$. At this temperature the largest eigenvalue of the structure factor matrix $S_{\alpha,\beta}(\mathbf{q})$ is nearly independent of the wave vector \mathbf{q} and is less than a factor of two larger than at $T = \infty$. Our values for the structure factor at this temperature are close to exact results for the ground state of a finite cluster with 36 sites.⁹ Our conclusions are summarized in Sec. IV.

II. SPECIFIC HEAT

The Hamiltonian of the Heisenberg model is given by

$$H = J \sum_{\langle i,j \rangle} \mathbf{S}_i \cdot \mathbf{S}_j, \quad J > 0, \quad (3)$$

where the sum runs over all pairs of nearest neighbors on the *kagomé* lattice. We calculated the high-temperature

TABLE I. For each quantity A we define the coefficients a_n by $A = \sum_{n=0}^{\infty} \frac{a_n}{n!} \left(\frac{\beta}{4}\right)^n$. The table shows the values of a_n for the specific heat C and the uniform susceptibility χ .

N	$4C$	4χ
0	0	0
1	0	4
2	48	-32
3	0	192
4	-9792	-384
5	0	-1280
6	4106880	-155136
7	-5193216	2711184
8	-2927834112	56705024
9	11470159872	-1716811776
10	3193027983360	-47711784960
11	-26121748561920	2004747075584
12	-4944246830899200	55843726884864
13	70892246893658112	-3367208347123712
14	10284867640404983808	-88720801213743104
15	-234226245436710912000	7723917022263705600
16	-27538523697287477329920	

series using a linked cluster expansion¹⁶ up to order 16 in $1/T$ (from now on we will set the exchange coupling J and the Boltzmann factor k_B equal to unity). The series coefficients are given in Table I. The series was extrapolated beyond its radius of convergence by the method of Padé approximants. For a power series $F(x)$ we form the Padé approximants

$$[L/M] = \frac{P_L(x)}{Q_M(x)}, \quad (4)$$

where $P_L(x)$ and $Q_M(x)$ are polynomials in x of order L and M respectively. The coefficients of the two polynomials are determined by the condition that the expansion of $[L/M]$ has to agree with the series $F(x)$ up to order $O(x^{L+M})$. Asymptotically a $[L/M]$ Padé approximant has the behavior

$$\lim_{x \rightarrow \infty} [L/M] \propto x^{L-M}. \quad (5)$$

In case of high-temperature expansions x is the inverse temperature. Because the specific heat must vanish at $T = 0$, we restrict the Padé analysis to approximants with $M > L$.

A number of approximants were obtained this way and are plotted in Fig. 2. The curves for different approximants remain consistent with each other down to $T = 0$. Furthermore, our findings agree with results from simulation studies on small clusters (of up to 18 sites).¹⁵ In particular there is only one peak at $T \approx 2/3$. We calculated the total change in entropy,

$$\Delta S = \int_0^\infty \frac{C}{T} dT, \quad (6)$$

and found

$$\frac{\Delta S}{N} \approx 0.6 \ln(2) \quad (7)$$

from integration of the Padé approximants for the spe-

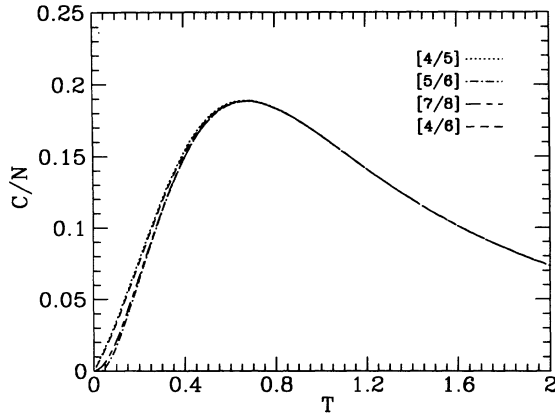


FIG. 2. $[L/M]$ Padé approximants for the specific heat C obtained from a 16-term high-temperature expansion.

cific heat. The $[L/L]$ Padé approximants for the entropy, which by construction go to a finite value at zero temperature, are in agreement with this result. Experiments on ^3He films¹⁴ absorbed on graphite reported a total change in entropy per site of about $\frac{1}{2} \ln(2)$. According to Elser,¹⁰ one quarter of the spins are essentially noninteracting, which, by themselves, give a zero-point entropy of $\frac{1}{4} \ln(2)$. The remaining three quarters of the spins form a *kagomé* lattice, so the experimental results¹⁴ predict a missing entropy of $\frac{1}{3} \ln(2)$ per site of the *kagomé* structure.¹⁷ This is close to our result that the missing entropy is approximately $0.4 \ln(2)$ per site. However, this is not enough to show that this model is appropriate to describe these experiments. There exist other proposals¹³ that give similar findings.

We do not, however, expect the large ground state degeneracy corresponding to a $T = 0$ entropy per site of $0.4 \ln 2$ implied by Eq. (7). Presumably tunneling removes the high ground state degeneracy which occurs in the classical model, leading to many low-lying (but split) states for the quantum case. This would give additional structure to the specific heat at low temperatures where the high- T series do not converge and where the experiments have not yet been performed.

We therefore also calculated the complete spectrum for finite systems with $N = 12, 15,$ and 18 sites using standard diagonalization routines.¹⁸ We chose two different clusters with 18 sites. The two possibilities, referred to as $18a$ and $18b$, respectively, are shown in Fig. 1. Cluster $18b$ is the one used in the exact-diagonalization studies by Zeng and Elser⁸ and the simulations performed by Fukamachi and Nishimori.¹⁵ Because translations are the only possible symmetry operations of this cluster, we were not able to reduce the dimension of the Hilbert space to a size that routines for complete diagonalization could be used. However, we calculated a large number of the low-lying eigenvalues by a Lanczos algorithm,¹⁹ which gives the accurate specific heat at the low temperatures of interest. Due to the larger symmetry of cluster $18a$, we were able to calculate all eigenvalues of this particular system as well as for the $N = 12$ and 15 clusters.

Results for the specific heat are presented in Fig. 3 together with one of the Padé approximants for com-

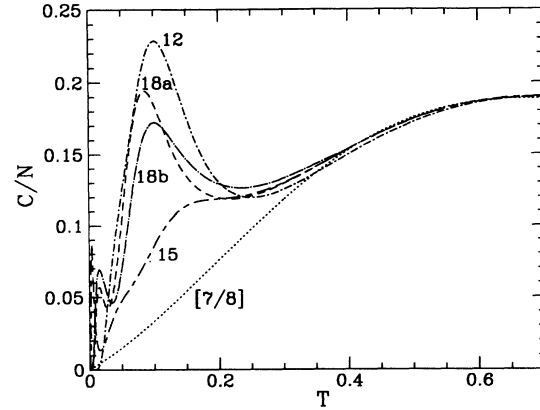


FIG. 3. The specific heat C calculated from exact-diagonalization of finite clusters compared with results from the Padé analysis of the high-temperature series. For cluster $18b$ only the low-lying eigenvalues have been determined and so the results are only presented for $T < 0.4$, the region where they are valid.

parison. The two different methods, high-temperature expansions in the thermodynamic limit and exact diagonalization for finite clusters, are in excellent agreement with each other down to $T \approx 0.3$, i.e., below the high-temperature peak. Thus, results from the finite cluster calculations are already in the thermodynamic limit for $T \geq 0.3$.

At lower temperatures, however, the two methods give completely different results. The finite clusters with an even number of sites develop a sharp peak in the specific heat, while the 15 -site system has at least a clear shoulder. In simulations¹⁵ the shoulder for the 15 -site system appeared to be much less significant and no peak was observed in the 18 -site system. This led to the conclusions that the low-temperature peak reported earlier¹⁰ was a finite size effect. Here we see that there *is* additional structure in the specific heat at low temperatures for larger sizes. We expect that some structure persists in the thermodynamic limit leading to a vanishing entropy as $T \rightarrow 0$. The precise form of this structure, e.g., broad shoulder or second peak, however, is difficult to deduce from our results, because the finite size corrections show a large even-odd asymmetry. Exact-diagonalization studies of finite clusters⁹ find that the lowest triplet (quadruplet) for finite systems with an even (odd) number of sites, N , has an excitation energy that remains finite in the thermodynamic limit resulting in a spin gap $\Delta \approx 0.25$. The low-lying states that give rise to the additional structure in the specific heat are singlets (doublets) for even (odd) N .

III. STRUCTURE FACTOR AND UNIFORM SUSCEPTIBILITY

In addition to the specific heat we also calculated the high-temperature series for the spin-spin correlations. Only 14 terms were determined for this series, because

many more clusters contribute to this expansion than for the specific heat. From the series for the correlations in real space we calculated the structure factor. As already mentioned in the Introduction the *kagomé* structure is not a Bravais lattice, and so the structure factor is a 3×3 matrix, given by

$$S_{\alpha,\beta}(\mathbf{q}) = \sum_{\mathbf{R}} \exp[-i\mathbf{q} \cdot (\mathbf{R} + \mathbf{b}_\beta - \mathbf{b}_\alpha)] \times \langle S^z(\mathbf{b}_\alpha) \cdot S^z(\mathbf{R} + \mathbf{b}_\beta) \rangle, \quad (8)$$

where \mathbf{R} is summed over Bravais lattice vectors formed from \mathbf{e}_1 and \mathbf{e}_2 in Eq. (1) and the \mathbf{b}_α , $\alpha = 1, 2$, or 3 are given by Eq. (2). Harris *et al.*⁷ showed that up to sixth order in $1/T$ the largest eigenvalue of this matrix is independent of the wave vector \mathbf{q} . This effect is due to the geometrical properties of the lattice. This degeneracy is broken in seventh order for quantum spins and in eighth order for the classical case. For certain values of the wave vector with high symmetry the eigenvectors are independent of T , and so the eigenvalues can be obtained as series in $1/T$. The results for the largest eigenvalue at $\mathbf{q} = 0$, $\mathbf{q} = \frac{2\pi}{3}(1, 0)$ (corner of the Brillouin zone) and $\mathbf{q} = \frac{\pi}{\sqrt{3}}(0, 1)$ (center of an edge of the Brillouin zone) are given in Table II. It is remarkable that the values for the different wave vectors differ by only about 5% indicating only weak dispersion. The \mathbf{q} value with the largest coefficient in the structure factor series changes at each order of the expansion; see Table II. This questions the conclusion in the classical limit,⁷ for which a tendency towards selection of $\mathbf{Q} = \frac{2\pi}{3}(1, 0)$ was reported based on an eight-term series. The next order of the expansion may already change that.

For wave vectors not at high symmetry points in the Brillouin zone we first calculated the Padé approximants for all nine matrix elements of $S_{\alpha,\beta}(\mathbf{q})$, evaluated them at a fixed temperature, and then diagonalized the matrix. In Fig. 4 we present results of a scan through the Brillouin zone at temperature $T = 0.25$. For these

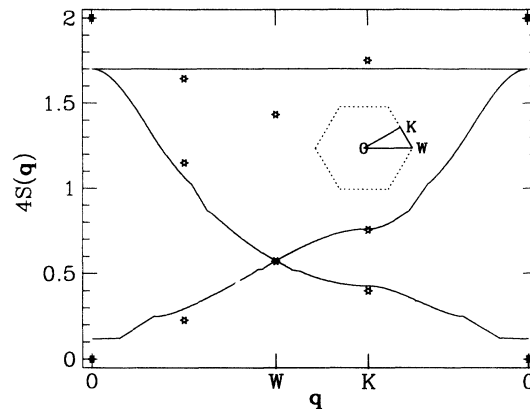


FIG. 4. The eigenvalues of the structure factor matrix at $T = 0.25$. The Padé analysis was done in the new variable $u = \tanh(f/2T)$ where $f = 0.125$. The asterisk marks the eigenvalues of the structure factor for the ground state of a finite cluster with 36 sites. The data were obtained using the results for the spin-spin correlations of this cluster given in Ref. 12.

data we first made a transformation to the new variable $u = \tanh(f/2T)$ where $f = 1/8$ and performed the Padé analysis in the series for this variable. We found that the transformed series behaved better than the original one. Figure 4 shows that the largest eigenvalue is nearly independent of \mathbf{q} . Although the different $[L/M]$ Padé approximants have a weak dispersion, there is no clear tendency towards selection of a particular \mathbf{q} value. We estimate that the largest eigenvalue of $S_{\alpha,\beta}(\mathbf{q})$ is given by

$$4S_{\max}(\mathbf{q}, T = 0.25) = 1.72 \pm 0.04, \quad (9)$$

and any dispersion is smaller than the error bars. For comparison, the corresponding result at $T = \infty$ is $4S_{\max} = 1$.

TABLE II. For each quantity A we define the coefficients a_n by $A = \sum_{n=0}^{\infty} \frac{a_n}{n!} \left(\frac{\beta}{4}\right)^n$. The table shows the values of a_n for the largest eigenvalue $S_{\max}(\mathbf{q})$ of the structure factor matrix at wave vectors $\mathbf{q} = (0, 0)$, $\mathbf{q} = \frac{\pi}{\sqrt{3}}(0, 1)$, and $\mathbf{q} = \frac{2\pi}{3}(1, 0)$.

N	$4S_{\max}(\mathbf{q}=0)$	$4S_{\max}[\mathbf{q} = \frac{\pi}{\sqrt{3}}(0, 1)]$	$4S_{\max}[\mathbf{q} = \frac{2\pi}{3}(1, 0)]$
0	1	1	1
1	2	2	2
2	4	4	4
3	-72	-72	-72
4	-448	-448	-448
5	11872	11872	11872
6	122368	122368	122368
7	-4503872	-4494912	-4493120
8	-61508608	-61640704	-61749760
9	3088187904	3072426496	3066299904
10	48686666752	49120629760	49365544960
11	-3348876193792	-3321064779776	-3305454742528
12	-54711166472192	-55953620766720	-56467096948736
13	5268689812606976	5210400086315008	5168484556144640
14	80271399635928064	84156994384281600	85379333782306816

In order to check whether our results give a correct picture of the low-temperature magnetic properties we calculated the structure factor for the ground state of a finite cluster with 36 sites. The ground state of this cluster has wave vector $\mathbf{q} = 0$. The correlations in real space are given in Ref. 12. For the 36-site system the allowed wave vectors are $\mathbf{q} = (0, 0)$, $\frac{\pi}{3}(1, 0)$, $\frac{2\pi}{3}(1, 0)$, $\frac{\pi}{\sqrt{3}}(0, 1)$, and others related by symmetry to these. The results are plotted in Fig. 4. The agreement between the results obtained from the series analysis at $T = 0.25$ and the ground state of the 36-site cluster is remarkable. It indicates that the results of the series analysis remain qualitatively unchanged down to $T = 0$; i.e., there is no divergence of the structure factor which would indicate magnetic order. The structure factor at $T = 0$ is roughly a factor of 2 larger than at $T = \infty$ and has only moderate dispersion, indicating a correlation length of less than one lattice spacing.

Results for the uniform susceptibility are plotted in Fig. 5 using the series for the susceptibility in Table I. We show only results for finite cluster with an even number of sites, N . As already mentioned at the end of the previous section the lowest states for a finite system with an odd number of sites are doublets which results in a strong finite size effect for the susceptibility: $\lim_{T \rightarrow 0} \chi = \frac{1}{4T} \frac{1}{N}$. Results from the high-temperature expansion and from finite cluster calculations again agree down to $T \approx 0.3$. Above this temperature the susceptibility is significantly smaller than the Curie-Weiss susceptibility. At low temperatures the susceptibility appears to vanish exponentially, because the low-lying states are all singlets. As mentioned earlier the spin gap Δ is estimated⁹ to be $\Delta \approx 0.25$. Because the $S^z = \pm 1$ components of the lowest triplet give identical contributions to the susceptibility, one expects the maximum in χ to occur at temperature $T_{\max} \approx \Delta/[1 + \ln(2)]$. This can be verified for the finite clusters with N sites by taking the finite size value $\Delta(N)$. The maximum for the susceptibility is given by $\chi_{\max} = 0.14-0.15$ with only a rather weak N dependence.

Experiments on ^3He films absorbed on graphite find a cusp in the susceptibility near 1 mK.²⁰ Unfortunately our data do not allow us to give quantitative estimates for the position and peak value of the susceptibility at such low temperatures, because the series expansion is no longer reliable and the finite cluster calculation suffers from finite size effects. It is very likely that in this temperature regime, $T \ll 1$, the spin- $\frac{1}{2}$ HAFM is no longer an appropriate model for ^3He films and additional interactions have to be taken into account.¹³

IV. CONCLUSIONS

We have presented results from high-temperature expansions and exact-diagonalization studies for the specific heat and the structure factor of the Heisenberg antiferromagnet on the *kagomé* lattice. Our main result is that the specific heat has additional structure a second peak or possibly a shoulder at very low temperatures in addition to a peak at higher temperature ($T \approx 2/3$). This had been conjectured earlier¹⁰ but sub-

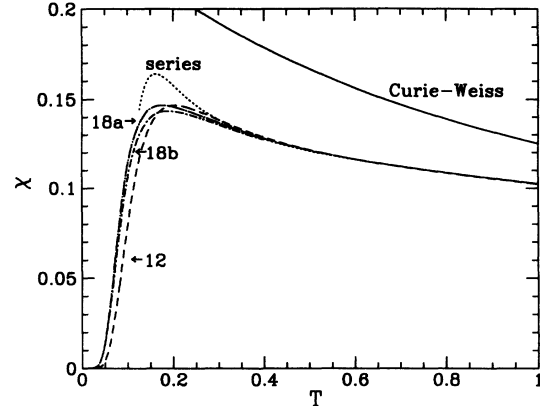


FIG. 5. Uniform susceptibility χ from finite clusters and a Padé analysis of the high-temperature series. The Padé analysis was performed for $T \ln(T\chi)$. The data shown were obtained from the [7/5] Padé approximant. The Curie-Weiss susceptibility $4\chi_{\text{CW}} = 1/(T - \Theta)$ with $\Theta = -1$ is shown for comparison. The first two terms in the high-temperature series expansions for χ and χ_{CW} are equal, and so $\chi \simeq \chi_{\text{CW}}$ at sufficiently high T .

sequent simulations¹⁵ had seemed to contradict it. Our conclusions that this unusual low-temperature behavior exists comes from the following observations: High-temperature series expansions, which do not find a second peak, obviously cannot account for a significant amount of entropy. At temperatures $T < 0.25$ finite cluster calculations show much more structures (a peak for even number of sites, N , a significant shoulder for N odd) in the specific heat. For $T \geq 1/4$ the results of both methods agree, showing that in this regime the finite cluster calculations give the correct results in the thermodynamic limit. Therefore, the specific heat below $T < 0.25$ has to be much larger than previously reported to get the entropy right, i.e., zero as $T \rightarrow 0$. Thus, what is seen in the finite cluster calculations is not a spurious finite size effect. It would be interesting to measure the specific heat at somewhat lower temperature to see if additional structure appears.

The series expansions for the structure factor at $T = 0.25$ give results that are very similar to the results for the ground state in exact-diagonalization studies.⁹ Both indicate that correlations fall off rapidly with distance. The structure factor is less than a factor of 2 larger the infinite temperature value even at $T = 0.25$. Any possible dispersion is too weak to be clearly identified. All this indicates that the Heisenberg antiferromagnet on the *kagomé* lattice has no long range magnetic order.

For the susceptibility we find a maximum around $T \approx \frac{1}{8}$ and an exponential drop at lower temperatures.

ACKNOWLEDGMENTS

One of us (N.E.) acknowledges support by the Deutsche Forschungsgemeinschaft. The work of A.P.Y. is supported by NSF Grant No. DMR 9111576.

- ¹ E. Manousakis, *Rev. Mod. Phys.* **63**, 1 (1991), and references therein.
- ² P. W. Anderson, *Mater. Res. Bull.* **8**, 153 (1973).
- ³ B. Bernu, C. Lhuillier, and L. Pierre, *Phys. Rev. Lett.* **69**, 2590 (1992).
- ⁴ P. W. Leung and K. J. Runge, *Phys. Rev. B* **47**, 5861 (1993).
- ⁵ R. R. P. Singh and D. Huse, *Phys. Rev. Lett.* **68**, 1766 (1992).
- ⁶ N. Elstner, R. R. P. Singh, and A. P. Young, *Phys. Rev. Lett.* **71**, 1629 (1993).
- ⁷ A. B. Harris, C. Kallin, and A. J. Berlinsky, *Phys. Rev. B* **45**, 2899 (1992).
- ⁸ C. Zeng and V. Elser, *Phys. Rev. B* **42**, 8436 (1990).
- ⁹ P. W. Leung and V. Elser, *Phys. Rev. B* **47**, 5459 (1993).
- ¹⁰ V. Elser, *Phys. Rev. Lett.* **62**, 2405 (1989).
- ¹¹ J. B. Marston and C. Zeng, *J. Appl. Phys.* **69**, 5962 (1991).
- ¹² S. Sachdev, *Phys. Rev. B* **45**, 12377 (1992).
- ¹³ M. Roger, *Phys. Rev. Lett.* **64**, 297 (1990).
- ¹⁴ D. S. Greywall and P. A. Busch, *Phys. Rev. Lett.* **62**, 1868 (1989); D. S. Greywall, *Phys. Rev. B* **42**, 1842 (1990).
- ¹⁵ K. Fukamachi and H. Nishimori, *Phys. Rev. B* **49**, 651 (1994).
- ¹⁶ M. P. Gelfand, R. R. P. Singh, and D. A. Huse, *J. Stat. Phys.* **59**, 1093 (1990).
- ¹⁷ We are grateful to Veit Elser for a discussion on this point.
- ¹⁸ W. H. Press, B. P. Flannery, S. A. Teukolsky, and W. T. Vetterling, *Numerical Recipes, The Art of Scientific Computing* (Cambridge University Press, Cambridge, England, 1986).
- ¹⁹ J. K. Cullum and R. A. Willoughby, *Lanczos Algorithms for Large Symmetric Eigenvalue Computations* (Birkhauser, Boston, 1985).
- ²⁰ M. Siqueira, C. P. Lusher, B. P. Cowan, and J. Saunders, *Phys. Rev. Lett.* **71**, 1407 (1993).